

Measuring Hemoglobin Levels in the Optic Nerve Head: Comparisons with Other Structural and Functional Parameters of Glaucoma

Manuel Gonzalez de la Rosa,¹ Marta Gonzalez-Hernandez,¹ Jose Sigut,² Silvia Alayon,² Nathan Radcliffe,³ Carmen Mendez-Hernandez,⁴ Julian García-Feijoo,⁴ Isabel Fuertes-Lazaro,⁵ Susana Perez-Olivan,⁵ and Antonio Ferreras⁵

PURPOSE. We evaluated and compared the ability of a new method for measuring hemoglobin (Hb) levels at the optic nerve head (ONH) to that of visual field evaluation, scanning laser ophthalmoscopy (HRT), scanning laser polarimetry (GDx), and optical coherence tomography (OCT) for diagnosing glaucoma.

METHODS. Healthy eyes ($n = 102$) and glaucomatous eyes ($n = 101$) underwent reliable Oculus Spark perimetry, and imaging with the HRT, GDx, and Cirrus OCT. In addition, ONH color images were acquired with a non-mydratic fundus camera. The Laguna ON_nE program then was used to calculate the Hb amount in each of 24 sectors of the ONH. Sensitivities at 95% fixed specificity, diagnostic agreement, and linear correlations between parameters with the best diagnostic ability were calculated.

RESULTS. The glaucoma discriminant function (GDF) of the Laguna program, evaluating Hb in the vertical intermediate sectors and center/periphery Hb amount slope, yielded an 89.1% sensitivity and 95.1% specificity, which was superior or similar to the other tests. The best GDF diagnostic agreement was for the OCT-vertical cup-to-disc (C/D) ratio ($\kappa = 0.772$) and the final phase Spark pattern SD ($\kappa = 0.672$). Hb levels correlated strongly with the Spark mean sensitivity (first phase 0.70, final phase 0.71). Hb also correlated well with the Reinhard OW Burk discriminant function of the HRT (0.56), nerve fiber indicator of GDx (−0.64), and vertical C/D ratio of OCT (0.71).

CONCLUSIONS. Hb levels evaluated by color analysis of ONH photographs had high reproducibility, a high sensitivity-specificity balance, and moderate to strong agreement with other structural and functional tests. (*Invest Ophthalmol Vis Sci.* 2013;54:482–489) DOI:10.1167/iovs.12-10761

The idea of measuring oxygen saturation in the retinal vessels is not new.^{1–7} Khoobehi et al. analyzed different points of the spectrum (hyperspectral analysis) to measure changes in oxygen saturation in anesthetized animals.⁸ From a practical point of view, Michelson et al. observed a reduction in arteriolar oxygen saturation of the optic nerve head (ONH) of eyes with low-tension glaucoma, but not those with primary open angle glaucoma (POAG) associated with ocular hypertension.⁹ Stefansson et al. observed that carbonic anhydrase inhibitors seem to increase oxygen saturation of the ONH.^{10,11} Although a subsequent investigation did not confirm this effect clearly,¹² the increased oxygenation induced by carbonic anhydrase inhibitors could be due to increased blood flow.¹³ Surgical reduction of ocular pressure seems to have no effect on ONH oxygenation levels.¹⁴ Recently, Denniss et al. captured hyperspectral images in human subjects *in vivo*.¹⁵ They observed that some differential light absorption values correlated well with visual sensitivity in POAG.

All these methods fail to take into account, however, the volume of blood in which the oxygen saturation is being evaluated. Tissue perfusion depends on various factors, such as blood volume, blood velocity, and the degree of oxygenation, but the reduction in oxygenation is moderate in glaucoma.⁹ Delori measured the reflectance spectrum of the ONH and studied the variables that affect the measurement of the existing blood volume.¹⁶ Sebag et al. estimated ONH blood volume in a cat,¹⁷ and Crittin et al. pointed out that reflectance changes at the ONH may be due to changes in the hemoglobin (Hb) amount.¹⁸

Although these three studies may be considered as the groundwork suggesting the possibility of measuring blood volume using reflectometry, they did not describe practical methods to measure the amount of Hb in the ONH in humans, compensating for lens absorption and diffusion, as well as changes in the intensity and spectral composition of the light used for illumination. We did not measure blood perfusion at the ONH. Our objective was to design a method, which we called the “Laguna ON_nE” (optic nerve hemoglobin), to measure the amount of Hb at the ONH using conventional fundus photographs that compensates for the aforementioned variables. The Laguna ON_nE may be used as an objective tool to differentiate between normal and glaucomatous optic neuropathy in clinical practice.

From the ¹Hospital Universitario de Canarias, University of La Laguna, La Laguna, Spain; the ²Department of Systems Engineering, University of La Laguna, La Laguna, Spain; the ³Weill Cornell Medical College, New York, New York; the ⁴Hospital Clinico San Carlos, University Complutense of Madrid, Madrid, Spain; and the ⁵Miguel Servet University Hospital, Aragon Health Sciences Institute, University of Zaragoza, Zaragoza, Spain.

Supported in part by Grant SolSubC200801000097 of the Agencia Canaria de Investigación, Innovación y Sociedad de la Información, and Grants PI09/0601 and PI11/01239 of the Instituto de Salud Carlos III, both with FEDER funds.

Submitted for publication August 13, 2012; revised October 28 and November 27, 2012; accepted December 3, 2012.

Disclosure: **M. Gonzalez de la Rosa**, P; **M. Gonzalez-Hernandez**, P; **J. Sigut**, None; **S. Alayon**, None; **N. Radcliffe**, None; **C. Mendez-Hernandez**, None; **J. García-Feijoo**, None; **I. Fuertes-Lazaro**, None; **S. Perez-Olivan**, None; **A. Ferreras**, None

Corresponding author: Antonio Ferreras, Department of Ophthalmology, Miguel Servet University Hospital, Isabel la Católica 1-3, 50009 Zaragoza, Spain; aferreras@msn.com.

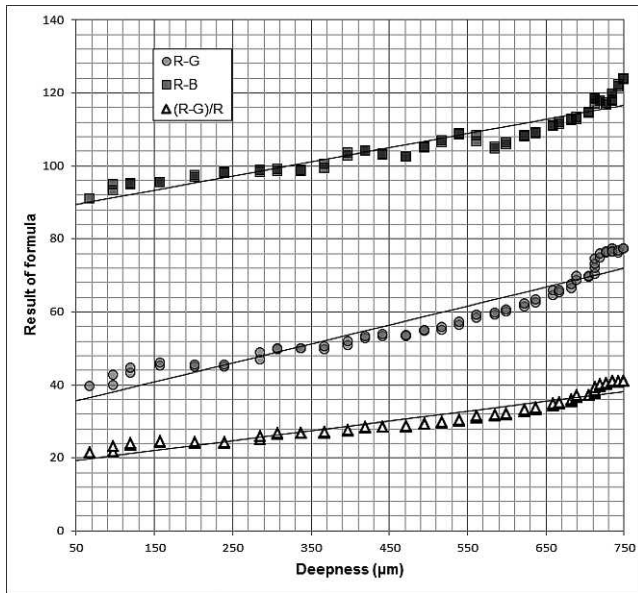


FIGURE 1. Results of different red (R), green (G), and blue (B) formulas obtained from a digital image of a variable deep bucket containing a hematite dilution. When the volume is small, there is a linear relationship between the RGB components, hemoglobin concentration, and bucket depth.

METHODS

The study protocol adhered to the tenets of the Declaration of Helsinki and was approved by the Institutional Review Board of the University Hospital of the Canary Islands. The participants were informed about the study objectives and signed informed consent was obtained from all of them.

A sample of 102 healthy eyes and 103 glaucomatous eyes were selected consecutively and prospectively. Normal eyes were recruited from patients referred for refraction who underwent routine examination without abnormal ocular findings, hospital staff, and relatives of patients in our hospital. Patients with glaucoma were enrolled from the Department of Ophthalmology of the University Hospital of the Canary Islands, Tenerife, Spain. One eye from each subject was chosen randomly for the study, unless only one eye met the inclusion criteria.

Eligible subjects had to have a best-corrected visual acuity of 20/40 or better, refractive error within ± 5.00 diopters equivalent sphere, and ± 2 diopters astigmatism, and an open anterior chamber angle. Individuals with diabetes or other systemic diseases that could affect vision or history of neurologic disease were excluded from the study. The presence of cataract was not considered a criterion for exclusion a priori. Age, and previous cataract and glaucoma surgery were not criteria for exclusion.

Study Protocol

Participants underwent a full ophthalmologic examination, including clinical history, visual acuity, biomicroscopy of the anterior segment using a slit-lamp, IOP measurement, and ophthalmoscopy of the posterior segment.

All glaucoma patients had perimetric assessment, having undergone at least two previous examinations. Normal subjects were examined twice, on successive days. The new white-on-white Spark strategy was used in an Easyfield perimeter (Oculus Optikgeräte GmbH, Wetzlar, Germany). The Spark strategy performs the examination in four phases. In the first phase, the threshold values are estimated on the basis of examining only six points.¹⁹⁻²¹ After this first phase, three more estimates are made. Finally, all points are examined one or more times. Once the four threshold estimates have been obtained, their median

TABLE 1. Demographic and Clinical Characteristics of Both Study Groups

	Control Group	Glaucoma Group	P
	Mean \pm SD	Mean \pm SD	
Age, y	54.5 \pm 17.4	52.9 \pm 16.6	0.25*
BCVA (Snellen)	0.99 \pm 0.05	0.93 \pm 0.14	<0.001*†
C/D	0.42 \pm 0.15	0.75 \pm 0.13	<0.001*†
MD of Spark			
perimetry, dB	0.38 \pm 0.90	-9.30 \pm 9.25	<0.001*†
PSD of Spark			
perimetry	1.42 \pm 0.24	4.50 \pm 3.00	<0.001*†
Sex, M/F	33/69	49/52	0.009†‡
N	102	101	

BCVA, best-corrected visual acuity; M/F = male/female; n = number of cases.

* Student t-test.

† P < 0.05 was considered statistically significant.

‡ χ^2 test.

value is calculated. An abnormal perimetry was defined as a reproducible glaucomatous visual field loss in the absence of any other abnormalities to explain the defect. A visual field loss was considered as a pattern standard deviation (PSD) elevated significantly beyond the 5% level.

Photographs of the optic disc were obtained using a Nidek AFC-210 non-mydiatic fundus retinograph (Nidek Co, Ltd., Gamagori, Aichi, Japan) and a Canon EOS 5D Mark II body camera (Canon, Inc., Lake Success, NY). Similar to the human eye, the sensor of a photographic camera does not read a single wavelength. It usually combines three image sensors that register polychromatic images, but with a preferred absorption for some short, medium, or long wavelengths. The Laguna ON_hE program analyzed three spectral components of ONH photographs: blue (B), green (G), and red (R). The ONH areas with high Hb content, mainly reflect red light. In contrast, areas with a low Hb content reflect a lower proportion of the red component compared to the green and blue light. Using different concentrations or different thicknesses of various red blood cell dilutions, it may be established experimentally that the photographic images obtained with this technique can be used to determine the amount of Hb. Based on the reflected amounts of red, green, and blue light, the results of several formulas, such as R - G, R - B, R - (G + B), (R - G)/R, R + B - (2G), (R - G)/G, etc., were almost linearly proportional to the amount of Hb present (Fig. 1).

The Laguna ON_hE program used mathematical algorithms for automatic component segmentation to perform a semiautomatic delimitation of the ONH border and to identify the central retinal vessels. Thus, two areas of the ONH were defined: the central retinal vessels and the ONH tissue itself. The formulas then were calculated at those pixels corresponding to the vessels as a whole and for every isolated pixel of tissue. The result obtained for the vessels was used as the reference value for calculating the Hb content in the tissue. For example, for the R - G formula, the R - G difference was calculated for the tissue, then divided by the R - G value for the vessels and the result was multiplied by 100.²² Finally, the influence of the lens status was compensated for by analyzing the differences between the green and blue components before calculating the results of the Hb amount. The blue, green, and red components were assessed with an image analysis program with the Matlab image processing toolbox (The MathWorks, Inc., Natick, MA).

Topographic analysis of the ONH was performed using a confocal scanning laser ophthalmoscope (HRT), the Heidelberg retina tomograph (HRT3; Heidelberg Engineering, Heidelberg, Germany). After keratometric readings were entered into the software, topographic images were obtained through undilated pupils and analyzed using the Advanced Glaucoma Analysis 3.0 software. All scans had to have an interscan SD of less than 30 μ m. The same glaucoma specialist traced

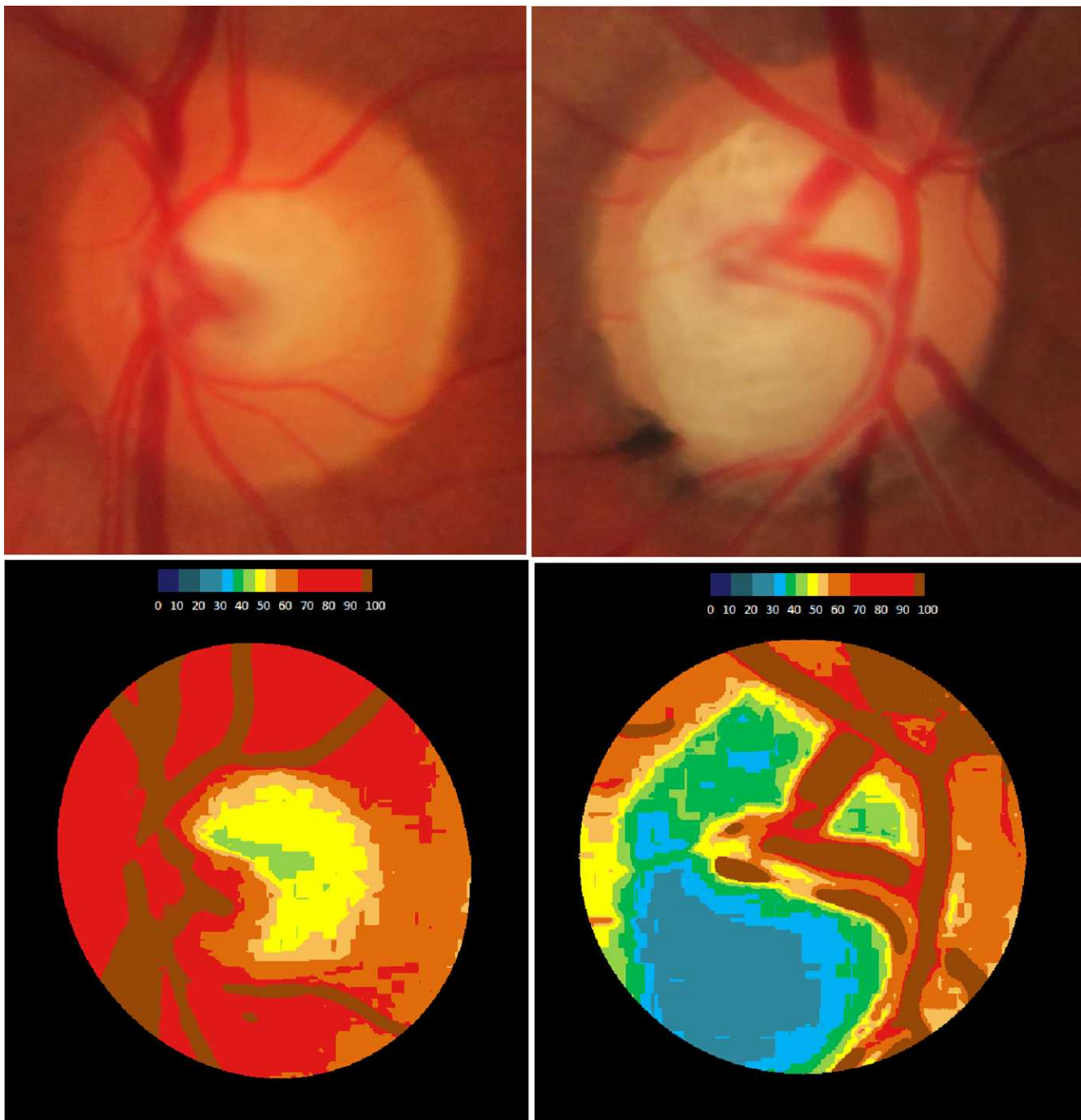


FIGURE 2. Examples of a normal (*left column*) and a glaucomatous (*right column*) papilla. *Upper images* are the color fundus photographs of the optic discs, while the *lower images* are their corresponding pseudo-images representing the amount of hemoglobin. A colorimetric scale is shown at the top of the lower images to assess the amount of Hb.

the margin of the optic disc, defining the inner edge of the Elschnig's ring with at least a four-point contour line.

The scanning laser polarimetries (GDx) were performed with the GDx-VCC (variable corneal compensation; Carl Zeiss Meditec, Dublin, CA). After macular scanning, the axis and magnitude of anterior segment birefringence were estimated from the measured macular retardation profile. Retinal polarization images then were obtained and compensated for automatically using the GDx-VCC software. At least one scan of acceptable quality (well focused and centered scans with a quality report ≥ 7) was obtained for each eye, and placement of the optic disc margin was confirmed by a trained ophthalmologist.

The peripapillary retinal nerve fiber layer (RNFL) thickness and ONH parameters (rim area, disc area, cup volume, mean cup-to-disc [C/D] ratio, and vertical C/D ratio) were measured using the optic disc cube 200×200 acquisition protocol (software version 5.2) of the Cirrus spectral-domain optical coherence tomography (OCT; Carl Zeiss Meditec). Left eye data were converted to a right eye format. All images were acquired with a quality greater than 6/10.

All the ophthalmic examinations, perimetry tests, and morphologic evaluation were performed within 1 month from the subject's date of enrollment into the study.

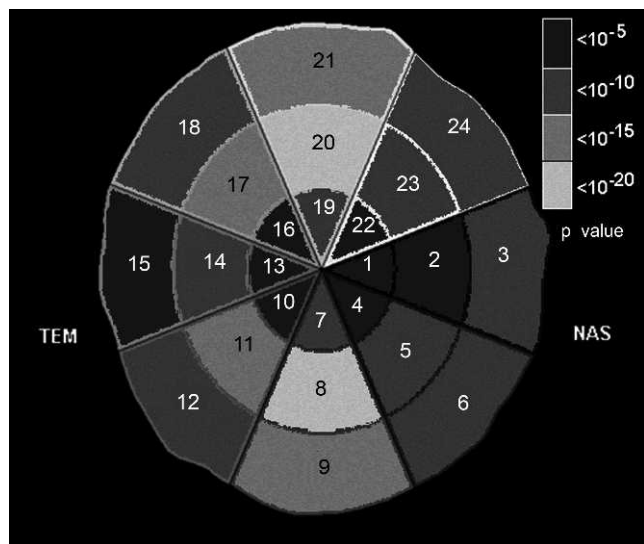


FIGURE 3. The image of the papilla was divided automatically into eight 45° radial sectors, and 2 concentric rings also were defined using 1/3 and 2/3 of the disc radius. Differences in Hb content in the 24 sectors of the optic disc (*P* value) between the group of normal subjects and the glaucoma group. NAS, nasal; TEM, temporal.

Classification into Groups

Healthy eyes had an IOP of less than 21 mm Hg, no history of increased IOP, normal optic disc morphology, and normal visual field results. The glaucoma group comprised subjects with POAG, pseudoexfoliative glaucoma, and pigmentary glaucoma. Glaucomatous eyes had focal (localized notching) and/or diffuse neuroretinal rim narrowing with concentric enlargement of the optic cup, and/or abnormal perimetry, regardless of the IOP values.

Statistical Analysis

All statistical analyses were performed using the IBM SPSS (version 17.0; IBM Corp., Somers, NY) statistical software and MedCalc (version 7.3; MedCalc Software, Mariakerke, Belgium). The areas under the receiver operating characteristic curves (AUCs) were calculated for all parameters of every test. Sensitivities at a fixed specificity of 95% (5% false positive rate) were compared between the parameters with the largest AUCs. Diagnostic agreement between the parameters with high diagnostic ability for each test was evaluated by the kappa statistic.

After checking for a normal distribution of the variables, Pearson correlations also were calculated between the structural and functional parameters.

RESULTS

One-eighth (12%) of the cases had associated cataracts, but only two cases with excessively blurred images were eliminated from the study. We analyzed 102 normal eyes and 101 eyes in the glaucoma group. Mean deviation (MD) ± SD of Spark perimetry was 0.38 ± 0.9 decibels (dB) in healthy subjects and -9.30 ± 9.3 dB in the glaucoma group (Table 1).

Figure 2 shows two examples of normal and glaucomatous papilla, and the corresponding pseudo-images indicating the Hb levels. Because ONH fundus photographs are two dimensional images, it is not possible to obtain automatically an accurate segmentation between the actual neuroretinal rim and the cupping. Thus, the whole optic disc was divided into 3 concentric rings, and each ring also was divided into 8 sectors (Fig. 3). The outer ring mostly aligns with the neuroretinal rim, the medium ring would be the transitional area, which may include the neuroretinal rim and cupping, and the inner rim mainly comprises the cup area. The vertical sectors showed the greatest difference in Hb amount between the healthy eyes and the glaucoma group, especially sectors 8 and 20 (*P* < 0.001). In particular, mean Hb amount in the pixels of these sectors (8 and 20) presented an AUC of 0.89, with 66% sensitivity at 95% specificity (*P* < 0.001, Table 2).

Mean Hb amount was calculated in: (1) sectors 9 and 21, (2) sectors 8 and 20, and (3) sectors 7, 10, 13, 16, and 19. Hb levels generally decreased from the periphery towards the center, that is from (1) to (3). Thus, the resulting slope correlated with the OCT vertical C/D ratio of 0.50 (*P* < 0.001). The Laguna ON_hE program uses an index called the Glaucoma Discriminant Function (GDF), which combines the slope of Hb amount with the mean in sectors 8 and 20. The GDF yielded 89% sensitivity at 95% specificity (*P* < 0.001, AUC = 0.97, Table 2).

Diagnostic agreement (kappa) between Hb-GDF, and the morphologic and functional parameters ranged between 0.474 for the Reinhard OW Burk (RB) discriminant function of HRT3, 0.672 for the final phase PSD of Spark, and 0.772 for the vertical C/D ratio of Cirrus OCT (Table 3). The poorest agreement between morphologic parameters was between the mean RNFL thickness of Cirrus OCT and the RB discriminant function of HRT3 (kappa = 0.553), while the best agreement was between the vertical C/D ratio of Cirrus and the global

TABLE 2. AUCs for Some of the Main Functional and Morphologic Parameters of the Evaluated Tests

	AUC	SE	Cut-Off Point	Specificity	Sensitivity	P Value
Spark MD phase 1	0.95	0.02	-0.7	96.1	85.1	<0.001
Spark PSD phase 1	0.87	0.03	1.7	95.1	66.3	<0.001
Spark MD final	0.96	0.01	-2.4	95.1	85.1	<0.001
Spark PSD final	0.97	0.01	1.9	95.1	82.2	<0.001
GDx NFI	0.82	0.03	27.1	95.1	57.1	<0.001
HRT RB	0.82	0.03	0.2	95.1	53.5	<0.001
HRT GPS	0.92	0.02	0.8	95.1	71.3	<0.001
OCT vertical C/D ratio	0.95	0.02	0.6	96.1	85.1	<0.001
OCT average thickness	0.88	0.02	76.4	95.1	67.0	<0.001
OCT superior thickness	0.87	0.03	88.1	95.1	64.4	<0.001
OCT inferior thickness	0.89	0.02	89.5	95.1	69.3	<0.001
Hb sectors 8+20	0.89	0.02	60.8	95.1	66.3	<0.001
Hb-GDF	0.97	0.01	0.0	95.1	89.1	<0.001

Specificity as close to 95% as possible was selected. The cut-off point value and sensitivities also were calculated. SE, standard error of the AUC; NFI = Nerve Fiber Indicator; GPS = global glaucoma probability score.

TABLE 3. Analysis of Diagnostic Agreement (Kappa) for Diverse Morphologic and Functional Parameters of the Different Tests Included in the Study Protocol

	Spark MD Final	Spark PSD Final	GDx NFI	HRT RB	HRT GPS	OCT Vertical C/D Ratio	OCT Average Thickness	Hb Sectors 8 + 20
Spark PSD final	0.910							
GDx NFI	0.488	0.586						
HRT RB	0.441	0.531	0.522					
HRT GPS	0.553	0.664	0.600	0.562				
OCT vertical C/D ratio	0.638	0.720	0.609	0.576	0.747			
OCT mean thickness	0.692	0.703	0.659	0.553	0.683	0.685		
Hb sectors 8 + 20	0.505	0.590	0.514	0.461	0.650	0.762	0.603	
Hb-GDF	0.627	0.672	0.526	0.474	0.660	0.772	0.619	0.629

Glaucoma Probability Score of HRT3 ($\kappa = 0.747$). The diagnostic agreement between MD and PSD Spark final phase was 0.910.

In the majority of cases when the value of Hb-GDF exceeded 0, at which point its specificity approaches 95%, the value of MD was higher than -3 dB. In many cases, however, when MD was lower than -3 dB, Hb-GDF clearly was abnormal (value lower than 0, Fig. 4). The same occurred with the other morphologic parameters. Mean Hb in sectors 8 and 20 was highly linearly correlated with functional and morphologic variables (Table 4), namely with the Spark mean sensitivity for the initial (0.70) and final (0.71) phases, and -0.59 and -0.62 with the respective values of PSD. Regarding HRT3, the correlation was 0.56 with the RB discriminant function and -0.68 for the glaucoma probability score. When the nerve fiber indicator of GDx was -0.64 , the mean RNFL thickness of OCT was 0.66 and the vertical C/D ratio was -0.71 . The correlation between the first (37 seconds) and final (2 minutes and 52 seconds) phases of Spark was 0.98 for MD and 0.96 for PSD.

Mean Hb in sector 8 had a correlation coefficient of 0.68 with Spark mean sensitivity of the upper hemifield, and mean Hb of sector 20 had a correlation coefficient of 0.69 with Spark mean sensitivity of the inferior hemifield. Although a linear regression analysis was performed, the relationship was linear

between the morphologic indices and Hb, and curvilinear between them and the perimetry values (Fig. 5).

The test-retest correlation in normal subjects was the same ($r = 0.96$) for Hb amount, vertical C/D ratio of OCT, and the nerve fiber indicator of GDx, but the coefficients of variation for these three indices were 3.0%, 5.5%, and 9.0% respectively.

DISCUSSION

Unlike other regions of the posterior pole of the eye, the ONH contains a significant amount of just one pigment, Hb, which is responsible for its particular color. Another peculiar feature of the ONH tissue observed with an ophthalmoscope or visualized with a fundus camera (retinograph) is a relatively thin layer over a white background, which comprises myelin surrounding the nerve fiber axons beyond the lamina cribrosa. For these reasons, the ONH color essentially depends on the Hb it contains.

Systems for fundus imaging measure the amount of light reflected at different wavelengths. For example, a detector that captures three images, one centered on spectral component blue, another on green, and another on red, reveals that in areas with high Hb content, most of the light reflected is red, less is green, and even less is blue. In contrast, in areas with a low Hb content, green and blue light is largely reflected.

When the intensity of reflected light is measured on a scale, for example from 0 to 255 (Fig. 6), the characteristics of each specific area of the image may be observed: arteries reflect more red, much less green, and even less blue (Fig. 6, row 1). Veins reflect less red than arteries, and very little blue and green at similar amounts, because the venous blood is less oxygenated (Fig. 6, row 2). Some tissue regions, which may have good perfusion, such as the neuroretinal rim, reflect more green and blue than the central retinal vessels, because they have less Hb (Fig. 6, row 3). Thus, in areas with atrophy or poorly vascularized tissue (excavation or cupping), the proportion of reflected G and B increases (Fig. 6, row 4), and this is perceived in the image as whitening.

To obtain absolute and reproducible results for the ONH, a reference pattern is needed because the results of the formulas depend not only on the amount of Hb, but also on the intensity and spectral composition of the illuminating light, and lens absorption, which mostly affects very short wavelengths (i.e., violet-blue) and to a lesser extent green. The reference value must be obtained inside the eye, and subject to the same variables. We found such a reference value, obtained from the central retinal vessels on their way through the ONH. Hb may be measured at each point or sector of the ONH using the same formula (F) to define the chromatic characteristics of the tissue (FT) and the reference vessels (FV). The amount of Hb at each point of the tissue is expressed as: $(FT/FV) \times 100$.²²

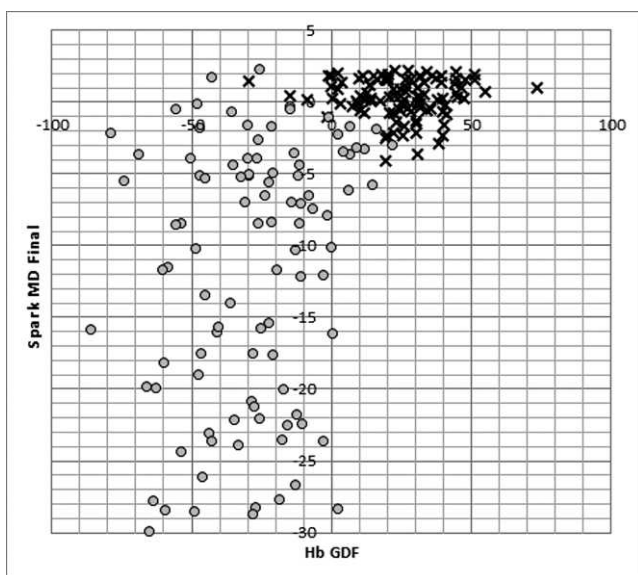


FIGURE 4. When the Hb-GDF was higher than 0, the MD of Spark perimetry generally was normal, but in some cases MD was normal and Hb-GDF was less than 0. Healthy subjects are represented by the *x*'s and glaucoma patients are represented by the *circles*.

TABLE 4. Linear Correlations between the Main Structural and Functional Parameters of the Studied Tests

	Spark MD Initial	Spark PSD Initial	Spark MS Final	Spark MD Final	Spark PSD Final	GDx NFI	HRT RB	HRT GPS	OCT Vertical C/D Ratio	OCT Avg. Thick.	Hb Sectors 8-20	Hb-GDF
Spark MS initial	0.984	-0.683	0.996	0.992	-0.732	-0.610	0.642	-0.616	-0.690	0.703	0.702	0.606
Spark MD initial		-0.702	0.983	0.972	-0.728	-0.588	0.633	-0.599	-0.662	0.680	0.698	0.587
Spark PSD initial			-0.688	-0.691	0.961	0.565	-0.473	0.576	0.582	-0.609	-0.595	-0.540
Spark MS final				0.996	-0.739	-0.616	0.640	-0.625	-0.691	0.711	0.714	0.617
Spark MD final					-0.745	-0.630	0.648	-0.648	-0.711	0.725	0.719	0.637
Spark PSD final						0.591	-0.520	0.609	0.619	-0.660	-0.623	-0.582
GDx NFI							-0.482	0.596	0.605	-0.671	-0.641	-0.602
HRT RB								-0.597	-0.629	0.578	0.561	0.469
HRT GPS									0.784	-0.675	-0.680	-0.692
OCT vertical C/D ratio										-0.685	-0.714	-0.703
OCT avg. thick.											0.660	0.631
Hb sectors 8-20												0.749

avg. thick., average thickness.

The loss of lens transparency due to cataracts, however, also produces diffusion of light in fundus images. This produces an increase in the green component of the vessels due to light coming from the tissue. These changes can be observed in the RGB histogram. In the vessels of patients with cataracts, the distance between the red and green components shortens, while the distance between blue and green increases. After cataract surgery, the blue value increases and the green value decreases as a consequence of the reduced diffusion, which increases the distance between red and green.

An equivalent phenomenon occurs in ONH tissue. In patients with cataracts, diffusion, and absorption of green and blue increase the distances between red and green, and between red and blue in the tissue. The diffusion of light from vessels also contributes to the increase of red in this tissue. If this is not corrected for, the relative redness of the image may lead to an overestimation of Hb content in the tissue. After cataract surgery, the differences between red and green, and between red and blue decrease, and, therefore, the area appears, correctly, whiter.

Because both effects of lens deterioration (on vessels and on tissue) are proportional, when measuring the differences between the distances of green and blue at the corresponding pixels to vessels, the extent of this absorption-diffusion effect on the tissue may be estimated. In this way, we can compensate for its effect on the Hb estimation.

Optic nerve perfusion basically depends on three factors: Hb content, blood flow rate, and oxygen saturation. When there are a few different types of tissue in the region of interest, and the intention is not to measure total perfusion but rather to determine oxygenation changes over time, it is useful to measure two or more wavelengths where oxy- and deoxy-Hb show the same and different absorbance. We believe that this measure of Hb content provides more information. This method had high reproducibility, good diagnostic capability, and diagnostic agreement with other morphologic procedures, similar to that when such procedures are mutually compared. ONH Hb correlated well with most of the morphologic and functional indices of POAG. Nevertheless, the high variability of normal human optic disc morphology (different disc sizes and distribution of the RNFL bundles in the ONH), as well as

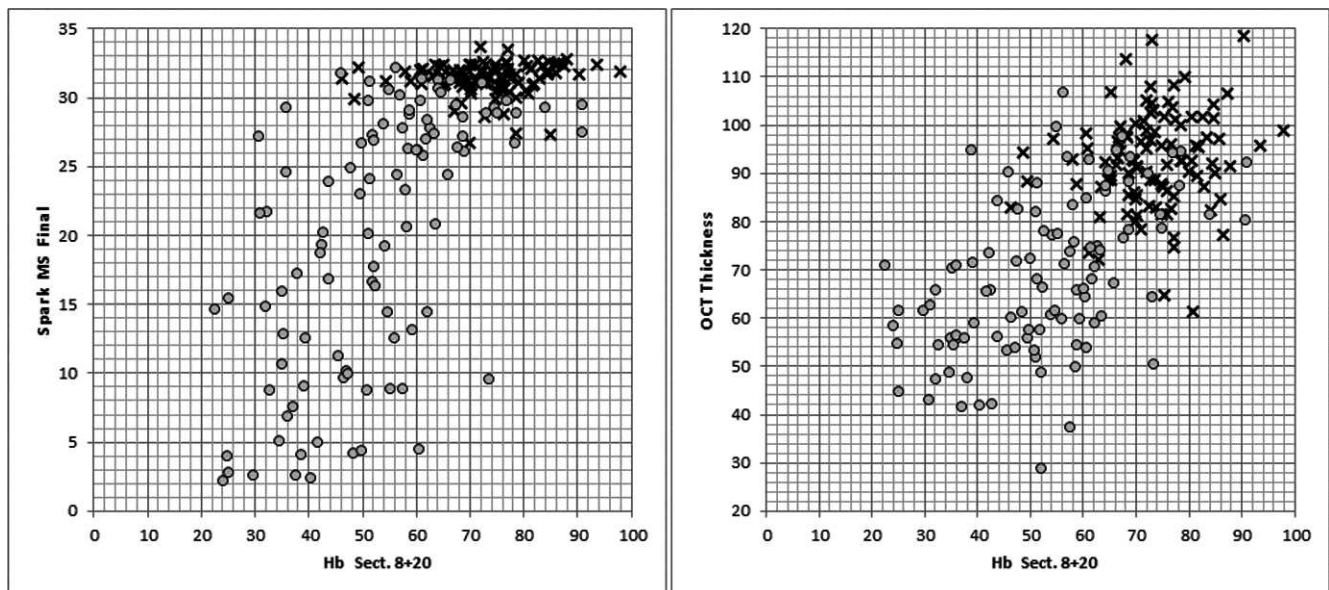


FIGURE 5. Relation between Hb content and mean sensitivity (MS) of Spark perimetry (left graph), and between Hb and mean RNFL thickness measured by Cirrus OCT (right graph). Healthy subjects are represented by the x's and glaucoma patients are represented by the circles.

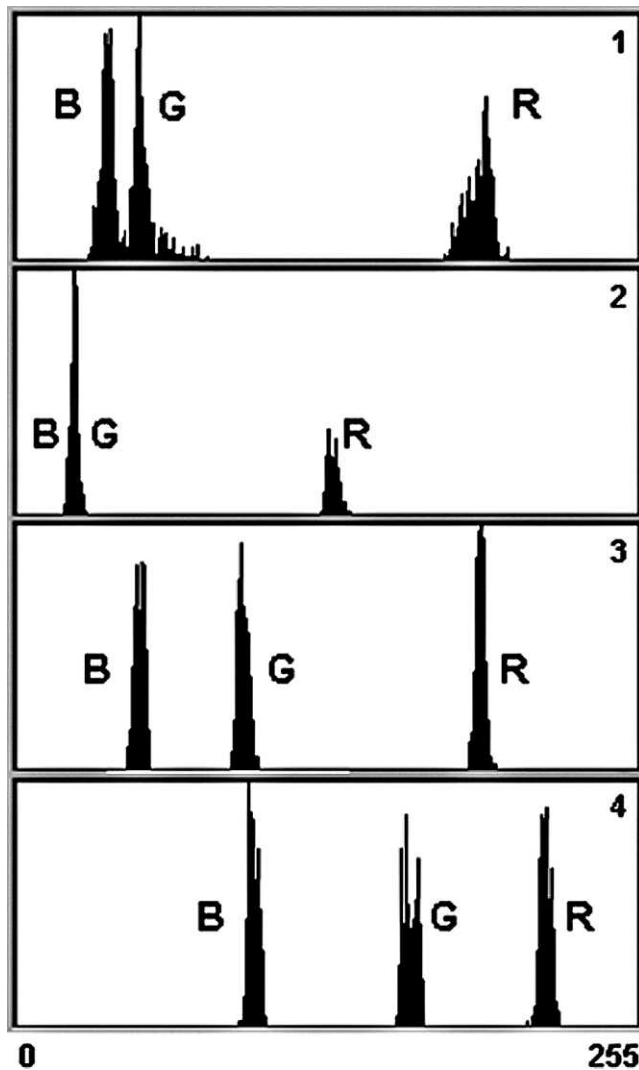


FIGURE 6. Histograms of the light component blue (B), green (G), and red (R) frequencies in different tissues, from a photographic image of a normal ONH. Each pixel in a digital image has a color produced by some combination of the primary colors (RGB). Each of these colors has a brightness value expressed as a number between 0 and 255 for a digital image with an 8-bit depth (x-axis). 0 corresponds to pure black and 255 corresponds to the maximum of the color. The y-axis represents the total number of pixels in the image with that level of brightness. Row 1: artery. Row 2: vein. Row 3: neuroretinal rim. Row 4: cupping.

refractive errors may affect measurement accuracy. Clinicians should take into account this limitation when using this method, as well as other imaging technologies, such as HRT, GDx, and OCT.

The authors of a recent study remarked that most of the techniques used to measure ocular blood flow (color Doppler imaging, confocal scanning laser ophthalmoscopic angiography with fluorescein and indocyanine green dye, laser blood flowmetry, scanning laser Doppler flowmetry, and retinal photographic oximetry) are not used habitually in clinical practice.²³ We believe that the availability of this new method, Laguna ON_hE, might change this tendency. The technique is relatively easy to apply and the majority of eye clinics already possess the required equipment, but each camera requires a specific correction of the function based on measurements acquired from a series of healthy subjects.

Laguna ON_hE also appears to have very promising applications in other lines of research. It remains to be demonstrated whether reduced perfusion precedes functional defects, tissue atrophy, and visual alterations. Although the diagnostic frequency of Hb-GDF suggests that this is so, long-term studies to verify this are required. Further, the method could be used to investigate whether perfusion changes are associated with IOP modifications (either medical or surgical), as well as early defects that then would lead to tissue atrophy and the corresponding functional defect. It also could be used to investigate possible perfusion defects of the optic nerve in patients with sleep apnea^{24,25} and the influence of hypercapnia on perfusion.²⁶

Our study may be the start of a new avenue of glaucoma research. These initial promising results should be confirmed and extended by other groups of investigators.

References

- Hickam JB, Frayser R, Ross JCA. Study of retinal venous blood oxygen saturation in human subjects by photographic means. *Circulation*. 1963;27:375-385.
- Laing RA, Cohen AJ, Friedman E. Photographic measurements of retinal blood oxygen saturation: falling saturation rabbit experiments. *Invest Ophthalmol Vis Sci*. 1975;14:606-610.
- Delori FC. Noninvasive technique for oximetry of blood in retinal vessels. *Appl Opt*. 1988;27:1113-1125.
- de Kock JP, Tarassenko L, Glynn CJ, Hill AR. Reflectance pulse oximetry measurements from the retinal fundus. *IEEE Trans Biomed Eng*. 1993;40:817-823.
- Beach JM, Schwenzler KJ, Srinivas S, Kim D, Tiedeman JS. Oximetry of retinal vessels by dual-wavelength imaging: calibration and influence of pigmentation. *J Appl Physiol*. 1999;86:748-758.
- Crittin M, Schmidt H, Riva CE. Hemoglobin oxygen saturation (So₂) in the human ocular fundus measured by reflectance oximetry: preliminary data in retinal veins. *Klin Monatsbl Augenheilkd*. 2002;219:289-291.
- Schweitzer D, Hammer M, Kraft J, Thamm E, Königsdörffer E, Strobel J. In vivo measurement of the oxygen saturation of retinal vessels in healthy volunteers. *IEEE Trans Biomed Eng*. 1999;46:1454-1465.
- Khoobehi B, Beach JM, Kawano H. Hyperspectral imaging for measurement of oxygen saturation in the optic nerve head. *Invest Ophthalmol Vis Sci*. 2004;45:1464-1472.
- Michelson G, Scibor M. Intravascular oxygen saturation in retinal vessels in normal subjects and open-angle glaucoma subjects. *Acta Ophthalmol Scand*. 2006;84:289-295.
- Stefánsson E, Jensen PK, Eysteinnsson T, et al. Optic nerve oxygen tension in pigs and the effect of carbonic anhydrase inhibitors. *Invest Ophthalmol Vis Sci*. 1999;40:2756-2761.
- Pedersen DB, Stefánsson E, Kiilgaard JF, et al. Optic nerve pH and PO₂: the effects of carbonic anhydrase inhibition, and metabolic and respiratory acidosis. *Acta Ophthalmol Scand*. 2006;84:475-480.
- Traustason S, Hardarson SH, Gottfredsdóttir MS, et al. Dorzolamide-timolol combination and retinal vessel oxygen saturation in patients with glaucoma or ocular hypertension. *Br J Ophthalmol*. 2009;93:1064-1067.
- Siesky B, Harris A, Kagemann L, et al. Ocular blood flow and oxygen delivery to the retina in primary open-angle glaucoma patients: the addition of dorzolamide to timolol monotherapy. *Acta Ophthalmol*. 2010;88:142-149.
- Hardarson SH, Gottfredsdóttir MS, Halldorsson GH, et al. Glaucoma filtration surgery and retinal oxygen saturation. *Invest Ophthalmol Vis Sci*. 2009;50:5247-5250.
- Denniss J, Schiessl I, Nourrit V, Fenerty CH, Gautam R, Henson DB. Relationships between visual field sensitivity and spectral

- absorption properties of the neuroretinal rim in glaucoma by multispectral imaging. *Invest Ophthalmol Vis Sci.* 2011;52:8732-8738.
16. Delori FC. Reflectometry measurements of the optic disc blood volume. In: Lambrou GN, Greve EL, eds. *Ocular Blood Flow in Glaucoma. Means, Methods and Measurements.* Berkeley, CA: Kugler and Ghedini; 1989:155-163.
 17. Sebag J, Feke GT, Delori FC, Weiter JJ. Anterior optic nerve blood flow in experimental optic atrophy. *Invest Ophthalmol Vis Sci.* 1985;26:1415-1422.
 18. Crittin M, Riva CE. Functional imaging of the human papilla and peripapillary region based on flicker-induced reflectance changes. *Neurosci Lett.* 2004;360:141-144.
 19. Gonzalez de la Rosa M, Reyes JA, Gonzalez Sierra MA. Rapid assessment of the visual field in glaucoma using an analysis based on multiple correlations. *Graefe's Arch Clin Exp Ophthalmol.* 1990;28:387-391.
 20. Gonzalez de la Rosa M, Hernandez Brito A, Quijada E. Campimetría para glaucoma explorando cuatro puntos. *Arch Soc Esp Ophthalmol.* 1992;62:93-98.
 21. Gonzalez de la Rosa M, Gonzalez-Hernandez M. A strategy for averaged estimates of visual field thresholds: Spark [published online ahead of print October 10, 2012]. *J Glaucoma.* doi: 10.1097/IJG.0b013e318239c1a3.
 22. Dill DB, Costill DL. Calculation of percentage changes in volumes of blood, plasma, and red cells in dehydration. *J Appl Physiol.* 1974;37:247-248.
 23. Harris A, Kagemann L, Ehrlich R, Rospigliosi C, Moore D, Siesky B. Measuring and interpreting ocular blood flow and metabolism in glaucoma. *Can J Ophthalmol.* 2008;43:328-336.
 24. Mojon DS, Hess CW, Goldblum D, Böhnke M, Körner F, Mathis J. Primary open-angle glaucoma is associated with sleep apnea syndrome. *Ophthalmologica.* 2000;214:115-118.
 25. Roberts TV, Hodge C, Graham SL, Burlutsky G, Mitchell P. Prevalence of nocturnal oxygen desaturation and self-reported sleep-disordered breathing in glaucoma. *J Glaucoma.* 2009;18:114-118.
 26. Hosking SL, Evans DW, Embleton SJ, Houde B, Amos JF, Bartlett JD. Hypercapnia invokes an acute loss of contrast sensitivity in untreated glaucoma patients. *Br J Ophthalmol.* 2001;85:1352-1356.